Electronic Supplementary Information

Multi-colour room temperature phosphorescence from fused ring compounds for dynamic anti-counterfeiting

Tongyu He [a]‡, Xueke Pang [a]‡, Airui Jiang [b]‡, Jiawei Zhang [a], Zhixia Feng [a], Wenxin Xu [a], Bin Song [a]*, Mingyue Cui [a]*, and Yao He [a]*

a. Suzhou Key Laboratory of Nanotechnology and Biomedicine, Institute of Functional Nano & Soft Materials & Collaborative Innovation Centre of Suzhou Nano Science and Technology (NANO-CIC), Soochow University, Suzhou 215123, China.

b. The First Affiliated Hospital of Soochow University, Soochow University, Suzhou 215006, Jiangsu, China.

* E-mail: bsong@suda.edu.cn; mingyuecui@suda.edu.cn; yaohe@suda.edu.cn

‡ Tongyu He, Xueke Pang, Airui Jiang, contributed equally to this work.

1. Experimental Section

Materials. Polyvinyl alcohol (PVA) (molecular weight (Mw) = 85,000 to 124,000 $gmol^{-1}$, 100% hydrolyzed), dimethylbenzene, benzo[a]phenanthrene (BZP), tetracene (TBZ), pyrene (PYR), and 1,2-benzanthracene (BZT) were purchased from *Sigma-Aldrich.* Poly(dimethylsiloxane) (PDMS) (Sylgard 184) were brought from Dow Corning Co., Ltd. Trichloromethane and alcohol were purchased from Sinopharm Chemical Reagent Co., Ltd (China). All the chemicals were used directly without further purification.

Optical characterization. Photoluminescence (PL) measurements were performed with a HITACHI F-4700 (Tokyo, Japan) fluorescence spectrofluorometer. Time-resolved phosphorescence emission spectra were recorded in transient spectrum system on Edinburgh FLS 1000 spectrofluorometer. The dynamics of emission decays were monitored by using the FLS1000's time-resolved single-photon counting multichannel scaling (MCS) mode with data collection for 5000 counts. Time-resolved fluorescence decay curves were attained on HORIB-FM-2015 spectrofluorometer with 370 nm lasers as the excitation source. Fluorescence microscopy images were measured by a fluorescence optical microscope (Leica, DM4000M, Germany) with a spot-enhanced charge couple device (Diagnostic Instrument, Inc.). The excitation source is a mercury lamp equipped with a band-pass filter (330-380 nm for UV-light, 400-450 nm for green-light). To determine $_{\Delta}E_{ST}$ values, low-temperature phosphorescence spectra of these four systems were measured at 77 K, based on the computational formula of $E=hc/\lambda$ (h: planck constant; c: light speed; λ: emission wavelength). The onset of fluorescence spectra at room temperature and phosphorescence spectra were used as the singlet and triplet energy levels, respectively.[1-2]

Pretreatment of the fused ring compounds (FRC). BZP, TBZ, PYR and BZT (50 mg for each molecule) were placed in four vials, and then 1 mL trichloromethane was dripped into the first three vials, and 1 mL xylene was dripped into the vial with BZT. The samples and solvents were mixed evenly and then left in a fume hood until all the solvents were volatilized.

Preparation of the PDMS elastic patterns. The polydimethylsiloxane (PDMS) film was produced by mixing prepolymer (Sylgard 184, Dow Corning) in a 10:1 base/curing ratio. The resultant sample was dried in a vacuum oven at 70 °C for 4 h. After cooling to room temperature, it was cut into the size of 1 cm × 1 cm.

Preparation of FRC@PVA. The procedure is described as follows. Firstly, BZP, TBZ, PYR and BZT (15mg for each molecule) after pretreatment were respectively dispersed in four vials of PVA solutions with the concentration of 30 mg mL^{-1}, and four homogeneous solutions were obtained after the

ultrasonication for 1 h. The solutions were swirled onto the PDMS patterns, after drying in air, the patterns were dried under 65 °C in an oven for 0.5 h, then cooled to room temperature. The FRC@PVA patterns with multi-colour phosphorescence emission were obtained for the anti-counterfeiting application.

2. Supplementary Figures

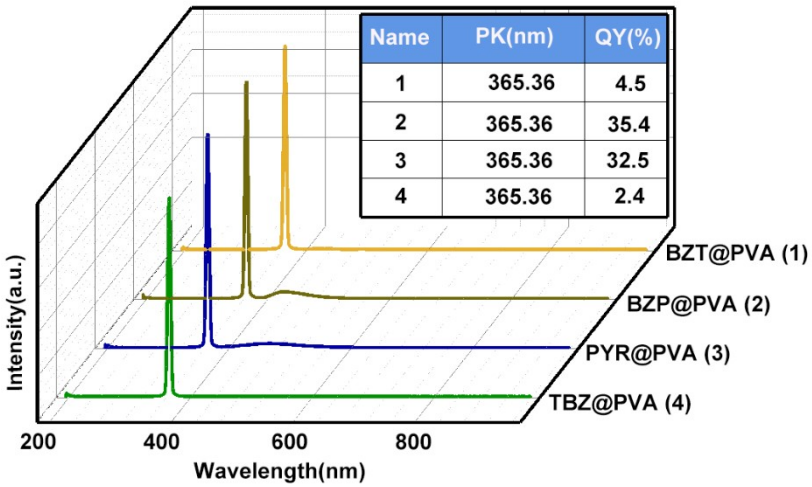

Figure S1. Quantum yield (QY) measurement of the FRC@PVA films.

The average QY values of the FRC@PVA films range from 2.4% to 35.4%. The highest QY can be observed in BZP@PVA (~35%), then in PYR@PVA (~32.5%). It demonstrates that the films of BZP@PVA, PYR@PVA exhibit strong fluorescence in air under irradiation.

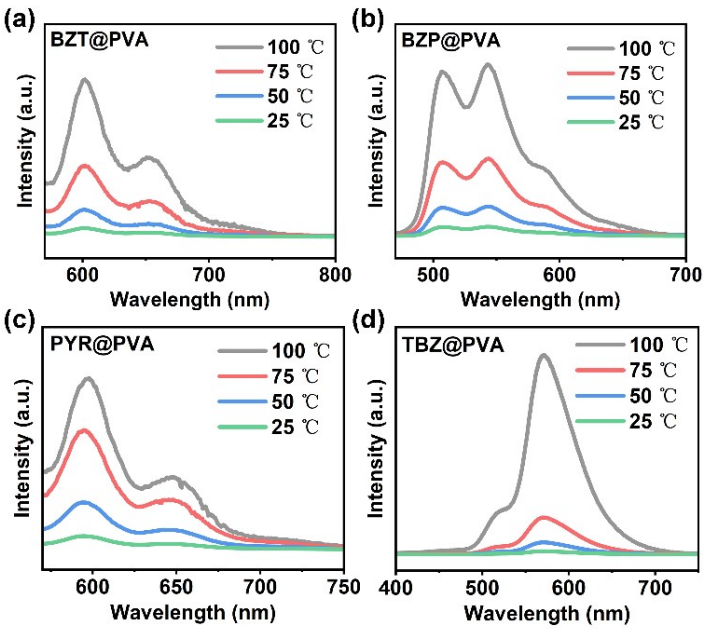

Figure S2. Phosphorescence spectra of FRC@PVA films under different reaction temperatures.

The reaction temperature is investigated towards the RTP properties in FRC@PVA films. the phosphorescence spectra prove that feeble phosphorescence emission is appeared when the initial reaction temperature is lower than 100 °C. As previous reported, the cross-linking between PVA molecular chains is promoted by increased curing temperature, producing stable network PVA films for preventing the quenching species.[3] Due to the heavy atoms or heteroatoms free composite in FRC, we deduce that the rigid matrix structures will dominate the RTP properties.

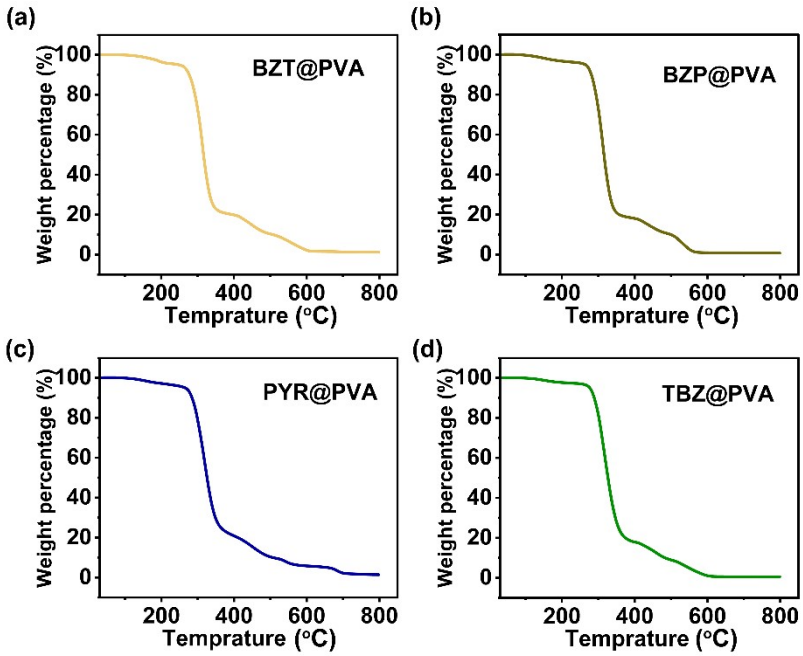

Figure S3. Thermogravimetric (TGA) profiles of FRC@PVA films. (a) BZT@PVA, (b) BZP@PVA, (c) PYR@PVA, (d) TBZ@PVA.

As shown in Figure S3, rapid mass loss between 300°C and 500°C is ascribed to the burning of carbonous residues. Comparatively, at 800°C, the residual weight percentage is nearly 0% for all FRC@PVA groups, owing to the pure organic system in this case.[4]

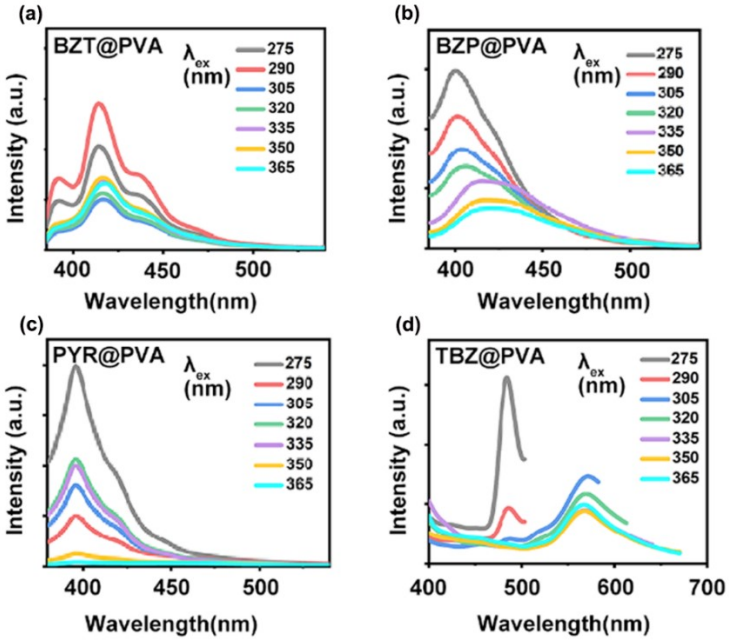

Figure S4. The fluorescence spectra of FRC@PVA films under serial excitation wavelengths from 275 to 365 nm. (a) BZT@PVA, (b) BZP@PVA, (c) PYR@PVA, (d) TBZ@PVA.

As depicted in Figure S4a, when the excitation wavelength ranges from 275 to 365 nm, the fluorescence emission peak of the BZT@PVA film remains constant at ~420 nm. Similarly, the emission peak of the PYR@PVA film remains unchanged with ~395nm (Figure S4c). However, there was a slight red shift of BZP@PVA films in emission peak as increasing excitation wavelength (Figure S4b). Additionally, a significant redshift is observed in Figure S4d for TBZ@PVA film.

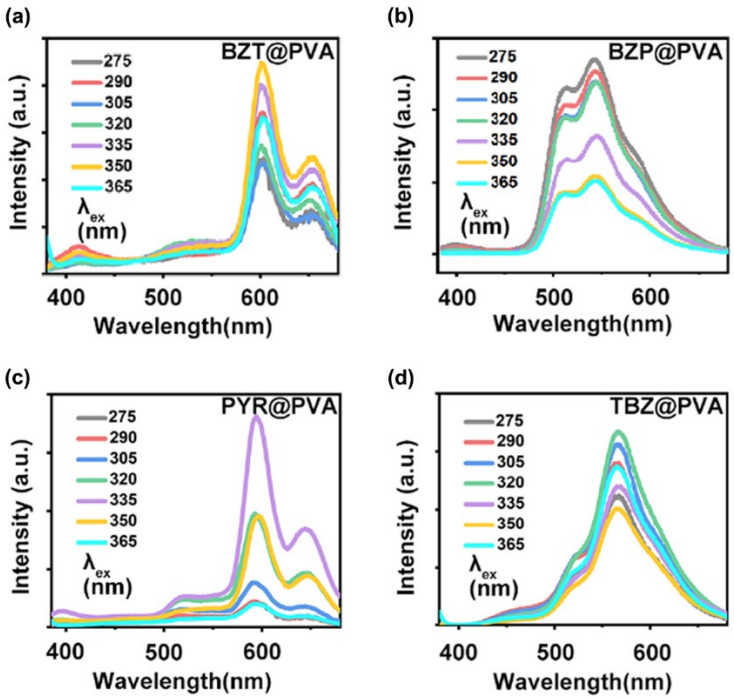

Figure S5. The phosphorescence spectra of FRC@PVA films under serial excitation wavelengths from 275 to 365 nm. (a) BZT@PVA, (b) BZP@PVA, (c) PYR@PVA, (d) TBZ@PVA.

As shown in Figure S5a-5d, upon increasing the excitation wavelength, the phosphorescence emission peaks of FRC@PVA films all keep constant without red shift, indicating that the phosphorescence of the films do not have the excitation-dependent characters.

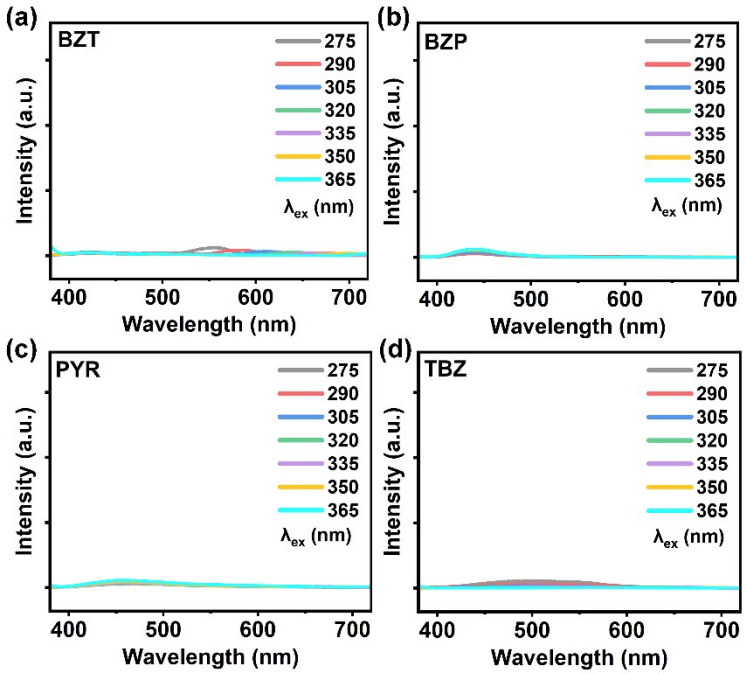

Figure S6. The phosphorescence spectra of FRC solutions under serial excitation wavelengths from 275 to 365 nm. (a) BZT, (b) BZP, (c) PYR, (d) TBZ.

As control groups, phosphorescence emission of pure FRC solutions is measured under various excitation wavelengths, barely phosphorescence signal can be detected in room temperature.

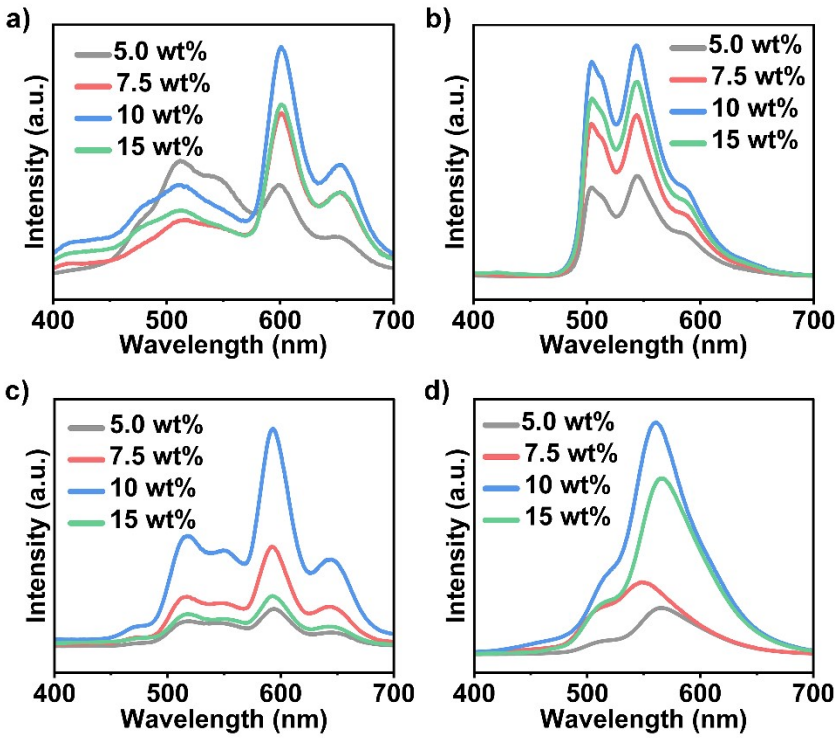

Figure S7. The phosphorescence spectra of FRC@PVA films with different doping ratios. (a) BZT, (b) BZP, (c) PYR, (d) TBZ.

Additionally, FRC@PVA films with different FRC doping ratios exhibit phosphorescence emission ranging from 500 to 650 nm. And the optimal phosphorescence intensity can be obtained under the doping ratio of 10 wt%.

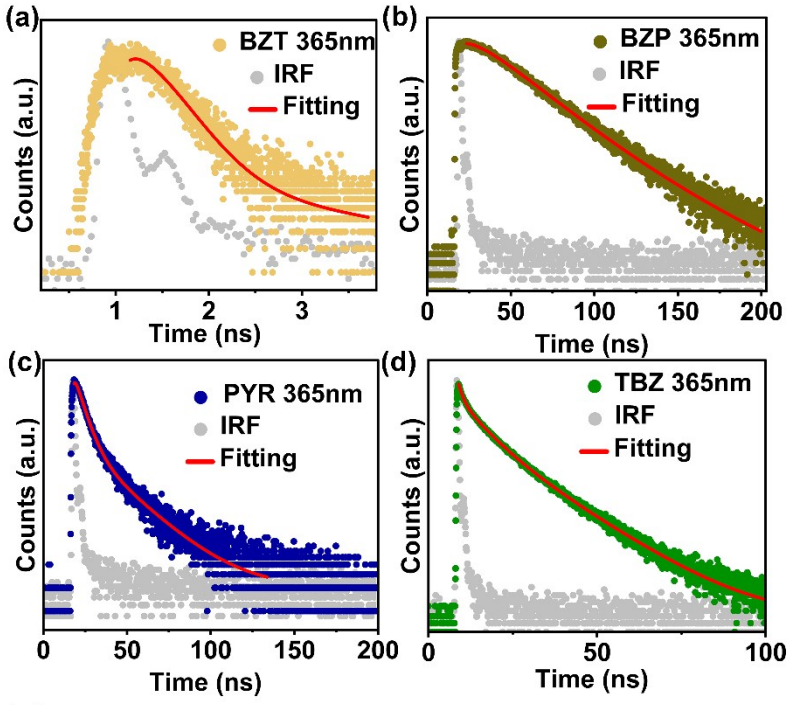

(e)

Name	BZT	BZP	PYR	TBZ
τ_{avg}/ns	3.35	35.19	11.92	9.90

Figure S8. Time-resolved fluorescence emission-decay curves of pure FRC solutions monitored at 365 nm. (a) BZT, (b) BZP, (c) PYR, (d) TBZ. (e) Fitting result of the fluorescence decay curves.

In time-resolved spectra, pure FRC with nanosecond lifetimes are calculated as 3.35ns (BZT), 35.19ns (BZP), 11.92ns (PYR) and 9.9ns (TBZ).

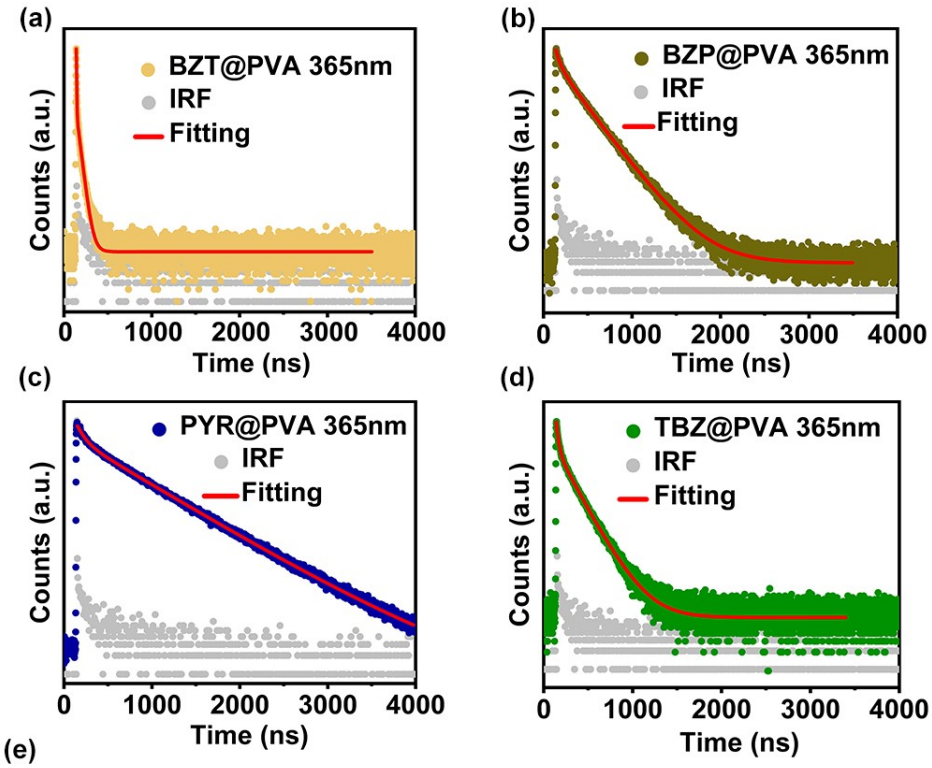

(e)

Name	BZT@PVA	BZP@PVA	PYR@PVA	TBZ@PVA
τ_{avg}/ns	1.35	102.74	46.46	16.20

Figure S9. Time-resolved fluorescence emission-decay profiles of FRC@PVA films monitored at 365 nm. (a) BZT@PVA, (b) BZP@PVA, (c) PYR@PVA, (d) TBZ@PVA. (e) Fitting result of the fluorescence decay curves.

The time-resolved fluorescence-decay curves were fitted to a tri-exponential function. BZP@PVA film show ultralong fluorescence lifetime of up to 102.74 ns, and the average fluorescence lifetimes of other FRC@PVA films are calculated to be 1.35 ns (BZT@PVA), 46.46 ns (PYR@PVA) and 9.3 ns (TBZ@PVA).

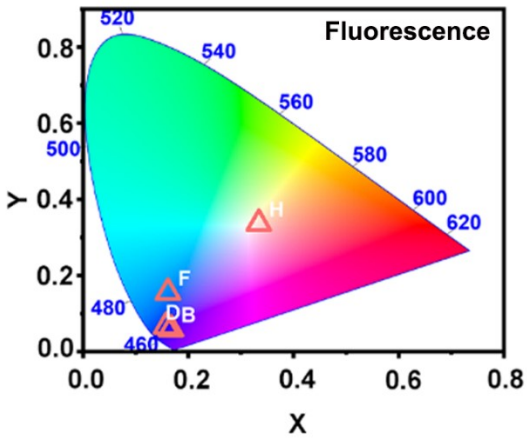

Figure S10. The fluorescence emission of the FRC@PVA films (B: BZT@PVA; D: BZP@PVA; F: PYR@PVA; H: TBZ@PVA) in CIE coordination plot.

Different from multi-colour phosphorescence, The CIE coordinates of the FRC@PVA films reveal only slight changes under 360 nm excitation. Only the TBZ@PVA is located in the yellow region (0.355, 0.324). The fluorescence emission of other FRC@PVA films (i.e., BZT@PVA, BZP@PVA, PYR@PVA) is observed in blue region, their CIE coordinates are (0.155, 0.042), (0.159,0.041) and (0.153, 0.092).

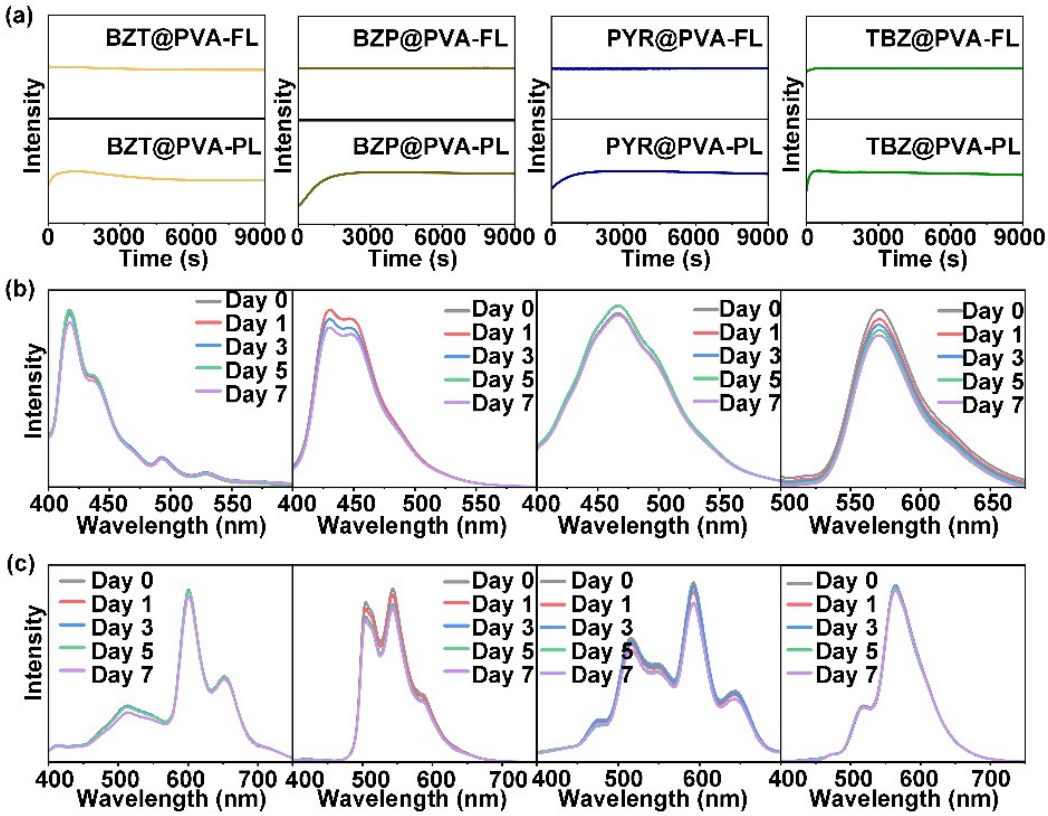

Figure S11. (a) Fluorescence (FL) and phosphorescence (PL) intensities spectra of BZT@PVA, BZP@PVA, PYR@PVA and TBZ@PVA films during 2.5 h UV irradiation. (b) FL and (c)PL spectra of BZT@PVA, BZP@PVA, PYR@PVA and TBZ@PVA films during 7 days storage.

The optical stability of four types of FRC@PVA films is investigated, revealing that the fluorescence and phosphorescence properties of these materials remain unchanged even after continuous ultraviolet light exposure for 2.5-hour and 7-day storage.

References

1. M. Y. Cui, M. J. Li, J.H. Wang, R. Z. Chen, Z. J. Xu, J. Y. Wang, J. F. Han, G. Y. Hu, R. Sun, X. Jiang, B. Song and Y. He, *Angew. Chem. Int. Ed.*, 2021, **60**, 15490.

2. M. Y. Cui, P. L. Dai, J. L. Ding, M. J. Li, R. Sun, X. Jiang, M. L. Wu, X. K. Pang, M. Z. Liu, Q. Zhao, B. Song and Y. He, *Angew. Chem. Int. Ed.*, 2022, **61**, e202200172.

3. J. W. Deng, H. Q. Liu, D. Y. Liu, Y. H. Bai, W. D. Xie, T. Q. Li, C. P. Wang, Y. F. Lian and H. L. Wang, *Adv. Funct. Mater.*, 2023, **34**, 2308420.

4. J. Escalante, W. H. Chen, M. Tabatabaei, A. T. Hoang, E. E. Kwon, K. Y. A. Lin and A. Saravanakumar, *Renew. Sust. Energ. Rev.,* 2022, **169**, 112914.